# Is brightfield all you need for MoA prediction?

Ankit Gupta†, Philip John Harrison†, Håkan Wieslander, Jonne Rietdijk, Jordi Carreras Puigvert, Polina Georgiev, Carolina Wählby, Ola Spjuth, Ida-Maria Sintorn

†These authors contributed equally to this work

NEURAL INFORMATION PROCESSING SYSTEMS

## Motivation

Fluorescence (FL) microscopy images from Cell Painting [1] provide invaluable information on the effects of drugs on cells. However, acquiring these images is expensive, time-consuming and labour-intensive, and the stains used can be cytotoxic. This is not the case for brightfield (BF) image acquisition, but due to low contrast the cellular compartments in BF images are difficult to differentiate. Nevertheless, harnessing deep learning, BF images may still be sufficient for various predictive tasks, such as predicting the mechanism of action (MoA) of different drugs.

## Explorations

We compared the predictive performance of ResNet-50 models trained on 20X images (2160x2160 pixels) for 231 compounds belonging to 10 MoA classes for BF data (6 z-planes) and FL data (5 fluorescence channels). For benchmarking purposes we trained fully-connected neural networks on CellProfiler (CP) features derived from the FL images. When DMSO solvent control data (i.e. no compound treatment) was included as a predictive class the BF models suffered (**Table 1a**), however, with the exclusion of this class the BF models actually outperformed both the FL and CP models (**Table 1b**).

**Table 1** Test set F1 score comparisons for the models trained on BF and FL images and CP features when **(a)** DMSO was included as a predictive class and **(b)** when it was excluded.

**(a)**

| | BF | FL | CP |
|---|---|---|---|
| ATPase-i | 0.674 | **0.701** | 0.699 |
| AuroraK-i | **0.742** | 0.675 | 0.677 |
| HDAC-i | **0.792** | 0.773 | 0.779 |
| HSP-i | 0.728 | **0.730** | 0.712 |
| JAK-i | 0.677 | 0.653 | **0.681** |
| PARP-i | 0.833 | 0.886 | **0.925** |
| Prot.Synth.-i | 0.768 | **0.793** | 0.770 |
| Ret.Rec.Ag | 0.684 | 0.769 | **0.795** |
| Topo.-i | 0.729 | 0.728 | **0.761** |
| Tub.Pol.-i | 0.881 | 0.854 | **0.887** |
| DMSO | 0.459 | **0.866** | 0.845 |
| Macro average | 0.724 | 0.766 | **0.776** |

**(b)**

| | BF | FL | CP |
|---|---|---|---|
| ATPase-i | **0.760** | 0.706 | 0.731 |
| AuroraK-i | **0.744** | 0.743 | 0.700 |
| HDAC-i | **0.800** | 0.785 | 0.772 |
| HSP-i | **0.744** | 0.708 | 0.716 |
| JAK-i | **0.756** | 0.671 | 0.705 |
| PARP-i | 0.890 | 0.878 | **0.960** |
| Prot.Synth.-i | **0.884** | 0.767 | 0.799 |
| Ret.Rec.Ag | 0.682 | 0.765 | **0.815** |
| Topo.-i | 0.733 | 0.715 | **0.771** |
| Tub.Pol.-i | **0.891** | 0.852 | 0.871 |
| Macro average | **0.788** | 0.759 | 0.784 |

For assessing reproducibility of a compound treatment and its perturbation strength relative to a DMSO control one can compute a grit score [2] (based on the CP features). **Fig. 2** shows the prediction accuracy against the grit score for the models with and without DMSO. The BF accuracy increased by 5% for compounds with lower grit scores (0-2) when DMSO was excluded, suggesting that removing the control class helps the BF models to better focus on compounds with more subtle morphological differences. The BF models also performed better than both FL and CP for compounds with a higher grit score (4-6).

Compound-level accuracy comparisons without DMSO are shown in **Fig. 3**. The compounds identified with blue crosses were either consistently better predicted by the BF models (5 compounds), compared to FL and CP models, or consistently worse (2 compounds). **Fig. 4** shows activation heatmaps (using guided backpropagation) for two of these "interesting" compounds that were better predicted by BF. The compound SR-1078 (BF accuracy = 0.933, FL accuracy = 0.167) is strongly activated in the BF heatmaps for vesicles that are not stained for in the Cell Painting protocol. That these vesicles should be important is supported by the fact that SR-1078 is known to target the retinoid receptor RORa which regulates lipid metabolism [3, 4]. For the compound DBeQ (BF accuracy = 0.800, FL accuracy = 0.033) there is overlap in the areas activated for BF and FL, however, for FL there is oversaturation in the signal, which could be hampering the predictive performance.

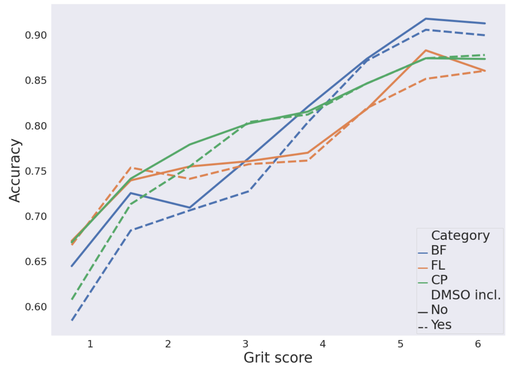


**Fig. 2** Comparison of accuracy at different grit scores for BF (blue), FL (orange), and CP feature-based (green) models across the test sets. The dotted lines represent the score when DMSO was included in the experiments and solid lines represent the results when DMSO was excluded.

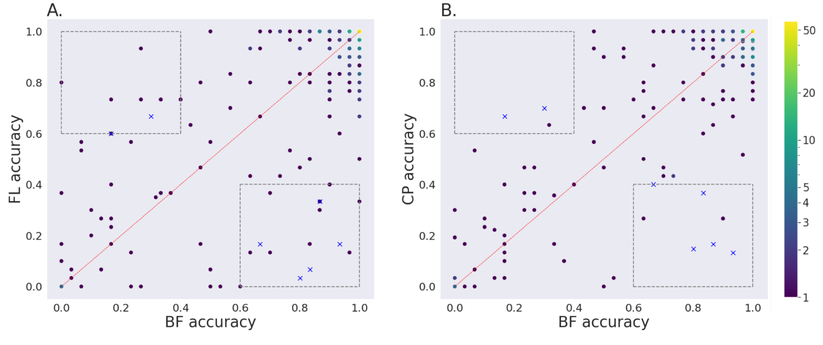


**Fig. 3** Comparison of the accuracy at the compound-level with the DMSO class excluded, across the test sets, for the BF models with respect to FL models, and CP feature-based models. Each dark dot represents a compound. Brighter dots represent multiple compounds with the same accuracy score. **A.** BF against FL. **B.** BF against CP. In the boxes at the bottom right and top left, thresholded at accuracy values of 0.6 and 0.4, the compounds shown with blue crosses were consistently better for BF than both FL and CP or consistently worse, respectively.

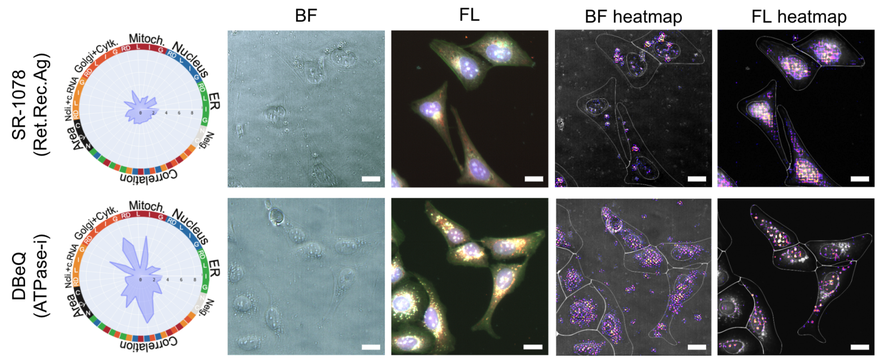


**Fig. 4** BF and FL images, activation heatmaps and radar plots for two compounds that were considerably better predicted by BF than both FL and CP models. The BF images show a maximum projection of the 6 z-planes. The FL images show a merge of the 5 channels with nuclei in blue, ER in cyan, RNA in grey, Golgi/F-actin in green and mitochondria in red. In the heatmaps the outlines of the nuclei and cells from CP are provided. The scale bars in the images represent 20 uM. The radar plots show the affected morphological features according to the CP data.

## Conclusions

We found comparable predictive performance for models based on BF images to those based on FL images and CP features. The BF models struggled more to separate the DMSO from compounds with subtler morphological differences, but performed better than the FL and CP models when DMSO was excluded as a predictive class. This may be explained by the fact that the brightfield images contain additional information for organelles not included in the Cell Painting protocol, such as the vesicles identified for the compound SR-1078. Hence, deep learning based features from BF images can be used to delineate compounds with different MoAs. This holds great promise for time-lapse studies, for which using FL data is problematic.

## References

[1]. Bray, MA. *et al.* (2016). "Cell Painting, a high-content image-based assay for morphological profiling using multiplexed fluorescent dyes". In: Nature Protocols 11, 1757–1774.

[2]. Trapotsi, M-A. *et al.* (2022). "Cell Morphological Profiling Enables High-Throughput Screening for PROteolysis TArgeting Chimera (PROTAC) Phenotypic Signature". In: ACS Chemical Biology 2022 17 (7), 1733-1744.

[3]. Wang, Y. *et al.* (2010). "Identification of SR1078, a synthetic agonist for the orphan nuclear receptors RORα and RORγ". In: ACS chemical biology, 5 (11), 1029-1034.

[4]. Kim, K. *et al.* (2017). "RORα controls hepatic lipid homeostasis via negative regulation of PPARγ transcriptional network". In: Nature communications, 8 (1), 1-15.

UPPSALA UNIVERSITET

HASTE

pharmb.io